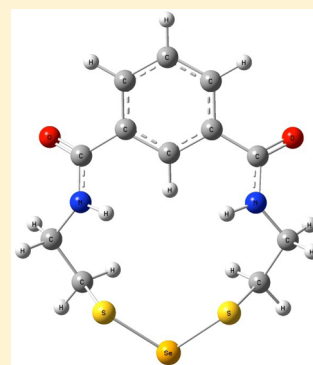


Removal of Selenite from Water Using a Synthetic Dithiolate: An Experimental and Quantum Chemical Investigation

Daniel Burriss,[†] Wenli Zou,[‡] Dieter Cremer,^{*,‡} John Walrod,[†] and David Atwood^{*,†}[†]Department of Chemistry, University of Kentucky, Lexington, Kentucky 40506-0055, United States[‡]Computational and Theoretical Chemistry Group (CATCO), Department of Chemistry, Southern Methodist University, Dallas, Texas 75275-0314, United States

Supporting Information

ABSTRACT: Combination of the dithiol *N,N'*-bis(2-mercaptoethyl)isophthalamide, abbreviated as BDTH₂ and as **1**, with excess H₂SeO₃ in aqueous acidic (pH ≈ 1) conditions resulted in precipitation of BDT(S–Se–S) (**6**), with a ⁷⁷Se NMR chemical shift of $\delta = 675$ ppm, and oxidized BDT. When the reaction is conducted under basic conditions Se(IV) is reduced to red Se(0) and oxidized **1**. No reaction takes place between **1** and selenate (Se(VI)) under acidic or basic conditions. Compound **6** is stable in air but decomposes to red Se(0) and the disulfide BDT(S–S) (**9**) with heating and in basic solutions. Mechanisms and energetics of the reactions leading to **6** in aqueous solution were unraveled by extensive calculations at the ω B97X-D/aug-cc-pVTZ-PP level of theory. NMR chemical shift calculations with the gauge-independent atomic orbital (GIAO) method for dimethyl sulfoxide as solvent confirm the generation of **6** (calculated δ value = 677 ppm). These results define the conditions and limitations of using **1** for the removal of selenite from wastewaters. Compound **6** is a rare example of a bidentate selenium dithiolate and provides insight into biological selenium toxicity.



1. INTRODUCTION

Selenium is an essential trace nutrient in biological systems, has antioxidant properties, and prevents the growth of a wide range of cancers.¹ There is a delicate ingestion balance, however, between selenium deficiency (<40 μ g/day) and toxicity (>400 μ g/day). Ingestion of excess selenium is harmful to the health of humans, wildlife, livestock, and aquatic organisms.² For this reason, the U.S. Environmental Protection Agency (EPA) limit for total selenium in drinking water is 50 ppb; in discharge, the EPA limit is 5 ppb to protect aquatic life in natural waters.³

Toxic concentrations of selenium are found in the wastewaters of steel mills, where the element is used for the production of machinable steels,^{4,5} or factories producing semiconductors, solar batteries, photoelectric cells, insecticides, fungicides, copper alloys, or glassware.² In these and other applications, it is desirable to remove high selenium concentrations from industrial wastewaters by a simple chemical process leading to a Se-containing precipitate that can be mechanically captured.

The synthetic, thiol-containing, metal capture agent *N,N'*-bis(2-mercaptoethyl)isophthalamide (abbreviated BDTH₂, based on the common name benzene-1,3-diamidoethanethiol) (Figure 1a) effectively precipitates soft divalent heavy metals such as cadmium, mercury, and lead from aqueous systems through the formation of covalent metal–sulfur bonds to form a BDT-metal precipitate.⁶ BDTH₂ irreversibly immobilizes mercury under a wide range of laboratory conditions,⁷ in gold mining effluent,^{8,9} acid mine drainage,¹⁰ and ppb levels of mercury in soil.¹¹ The BDT(S–Hg–S) compound that forms

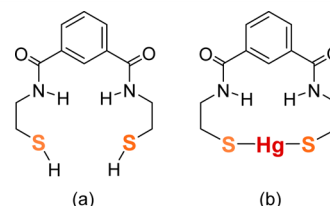


Figure 1. (a) BDTH₂ and (b) BDT(S–Hg–S).

under these conditions (Figure 1b) does not release mercury under strongly acidic or basic conditions.¹²

Additionally, BDTH₂ has a very high oxygen-radical-adsorbance capacity (ORAC) of 192 400 μ mol/100g (Acai = 18 500), is without toxicity when administered in test animals (LD₅₀ > 5 mg/kg body mass), and removes 90% intracellular mercury.¹³ In one study BDTH₂ protected rats when injected with mercury at 5 times the lethal dose.¹⁴

Extensive calculations on the Hg–S bonds within BDT–Hg determined a characteristic strong bond dissociation enthalpy (BDE) of 68 kcal/mol.¹⁵ Given that the Se–S BDE for HSSeH is 59 kcal/mol and increases by 5 kcal/mol when the hydrogens are replaced by alkyl groups (this work), it was anticipated that BDTH₂ might precipitate selenium from aqueous solutions and find utility in removing selenium from industrial wastewaters.

In contrast to mercury, however, the interaction of thiols with selenite is much more complex and involves reduction of

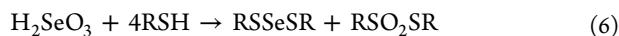
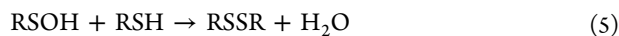
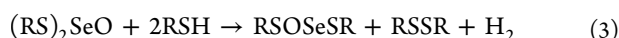
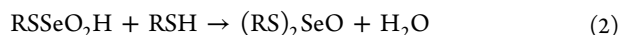
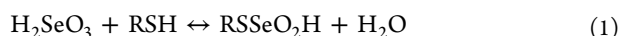
Received: November 26, 2013

Published: April 2, 2014

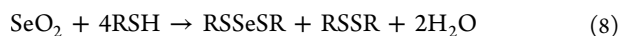
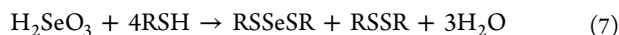
Se(IV) to Se(II) and ultimately to Se(0) (see reactions 1–9). It is well-established that the interaction of Se(IV) with alkane thiols results in the formation of disulfides and various selenium-containing intermediates before ultimate reduction to elemental Se(0).^{16–18} These reactions depend on pH, the availability of excess thiol, and ligand sterics (reactions 1–6).^{17–19} Reactions 1–3 are typically too rapid to allow isolation of the intermediate selenium compounds, and the selenium(II)dithiolate RS–Se–SR (reaction 4) is the most commonly observed product. The overall reaction between Se(IV) and 4 equiv of thiol can be written as in reaction 7 or 8 as was first described in 1941.¹⁶ In the presence of 2 additional equiv of thiol, Se(II) is reduced to Se(0) (reaction 10). The Se(II) compounds are unstable, and even without additional thiol, readily decompose to Se(0) and disulfide with heating or in neutral to basic solutions (reaction 11).

The toxicity of selenium must be due, in part, to the ease with which Se(IV) oxidizes the sulfhydryl groups of cysteine and particularly glutathione.²⁰ Compounds of the form RS–Se–SR (with R = cysteine, glutathione, or coenzyme A) are important intermediates in the incorporation of inorganic selenium into living systems.¹⁹

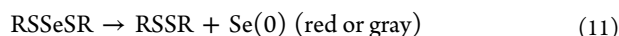
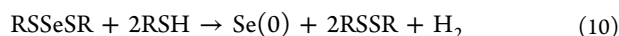
Reactions of Se(IV) with Thiols.



Overall Reactions:

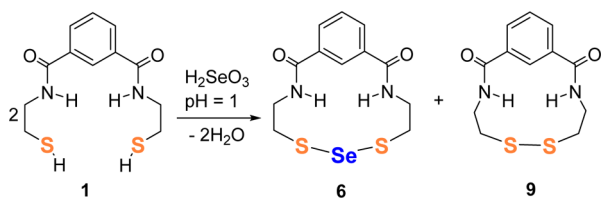


Decomposition Reactions



This publication will explore the interaction of selenite with **1**, a compound with two cysteamine groups (see Scheme 1), through experimental and computational techniques. BDT(S–

Scheme 1. The Combination of BDTH₂ (1**) and Se(IV) to Form BDT(S–Se–S) (**6**) and BDT(S–S) (**9**)^a**



^aThe eight potential reaction intermediates **2**, **3**, **4**, **5**, **7**, **8**, **10**, and **11** leading to **6** and **9** are shown in Scheme 2 along with two forms of oxidized BDT in addition to **9**.

Se–S) (**6**) is the ultimate selenium-containing compound in this reaction and, although prone to decomposition, is sufficiently stable to be characterized. A comprehensive computational analysis is presented on the potential reaction intermediates **2–5** and **7–11** (see Scheme 2) that may exist leading to **6**, including the BDT analogs of the general compounds implicated in reactions 1–6. The utility of **1** as a sequestration agent for aqueous selenium will be critically evaluated. As a bidentate thiol, BDTH₂ provides insight into the interaction of selenium with proteins that utilize cysteine to form disulfide linkages.

2. RESULTS AND DISCUSSION

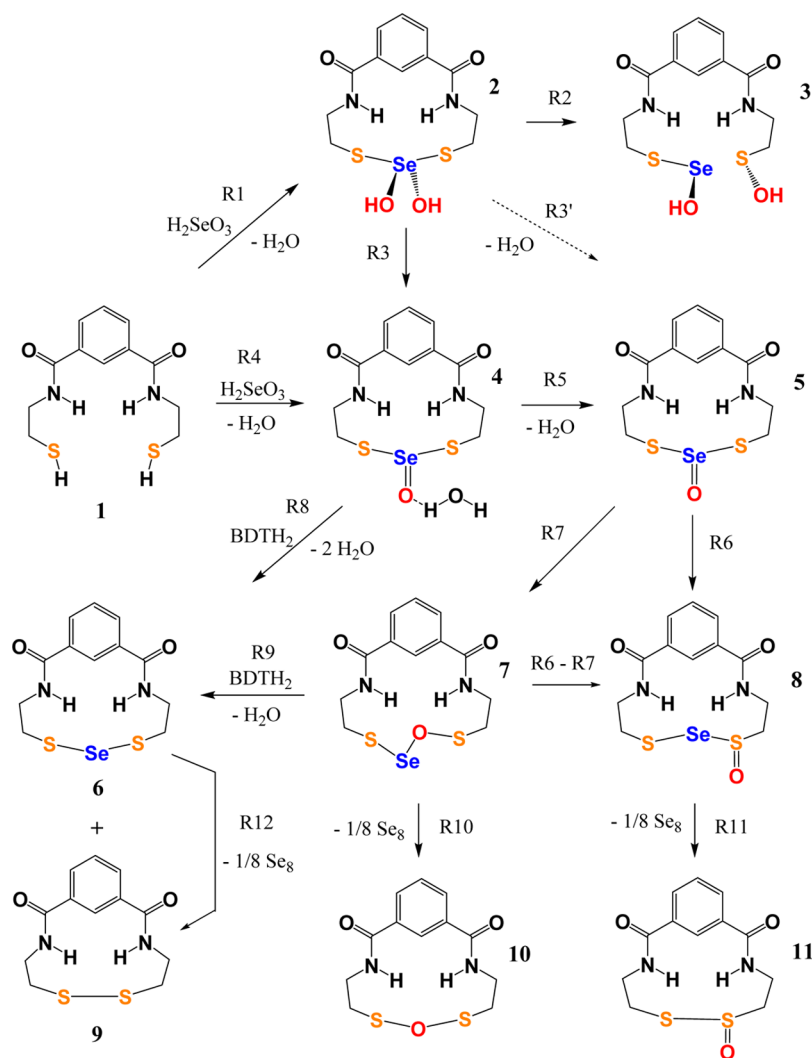
2.1. Synthesis and Characterization of BDT(S–Se–S) (6**).** The combination of selenite, as H₂SeO₃, with BDTH₂ (**1**) was explored with equimolar and excess amounts of the reagents in acidic or basic aqueous solutions. Red elemental selenium, Se(0), immediately formed in neutral to basic solutions when either reactant was used in excess. There is substantial literature precedent for this reaction as red Se(0) was also observed when selenite was combined with cysteine, mercaptoethanol,¹⁶ various butanethiols,¹⁸ thioglycolic acid, mercaptopropionic acid,²¹ and glutathione¹⁷ under neutral or basic²¹ conditions.

Under acidic conditions, excess BDTH₂ and selenite produced a yellowish solid that agglomerated into a spherical, hard solid that was difficult to handle. The ¹H NMR spectra revealed the product to be a mixture of BDT-containing compounds. Moreover, gray elemental selenium precipitated when this product was dissolved in DMSO-*d*₆.

The best synthetic method to prepare **6** was to add BDTH₂ dropwise, over the course of several hours, to an acidic (pH ≈ 1) aqueous solution containing 2 equiv of selenite. A pale yellow solid precipitated immediately after combining the two reagents. BDT(S–Se–S) (**6**) was the only selenium-containing product but contained coprecipitated BDT(S–S) (**9**) due to oxidation of **1**. This reaction proceeded in a similar manner to those conducted under neutral and basic conditions but without visual evidence of red Se(0). The product was insoluble in water and common organic solvents (such as acetone, ethanol, hexane, methanol, etc.) but soluble in DMSO and pyridine. However, dissolution in either of these two solvents resulted in decomposition of **6** to red Se(0).

The instability of **6** in basic solutions was used to isolate **9** from the precipitated mixture. The mixture containing **6** and **9** was dissolved in DMSO to form a clear yellow solution. A red DMSO layer containing Se(0) and **9** formed above a clear saturated basic layer upon the addition of saturated aqueous sodium hydroxide. The clear bottom layer was removed, and centrifugation caused precipitation of a yellow-white precipitate from the red solution. The precipitate was isolated and then extracted with 1,3-diaminopropane to extract elemental selenium from the solution. This procedure was repeated until **9** was obtained as a white solid and characterized. The infrared (IR) spectrum had absorptions characteristic of NH (3238 cm^{–1}), C=O (1636 cm^{–1}), and C–H groups (sp² and sp³). In the Raman spectrum the disulfide peak of BDT(S–S) (**9**) was found at 511 cm^{–1}. This is very similar to the peak at 510 cm^{–1} found for the disulfide in cystamine dihydrochloride (cystamine disulfide).²² The spectroscopic data did not contain peaks associated with sulfonic or sulfonate groups; for example, no peaks similar to 540 cm^{–1} in MeSO₃H or 578 cm^{–1} in MeSO₃Na were observed.²³

Scheme 2. Potential Reaction Steps, R1–R11, for the Combination of BDTH₂ (1) with H₂SeO₃ to Precipitate a Mixture of BDT(S–Se–S) (6) and BDT(S–S) (9) from Water



With S–Se–S bonding, **6** corresponds to the selenium dithiolate, RS–Se–SR, in reactions 4, 6, 7, and 8 (Scheme 2). However, **6** is a rare example of such a compound with a bidentate thiolate. The only other examples of selenium with bidentate thiolates are two lipoic acid derivatives, which are uniquely stable compared to other selenium dithiolates (Figure 2).²⁴ The compounds do not appreciably decompose in

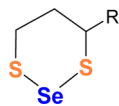


Figure 2. Bidentate selenium dithiolates with lipoic acid derivatives (R = (CH₂)₄COOH and (CH₂)₄CONH₂).

aqueous solution until pH > 7.5, and 80% MeOH–TFA solutions decompose by only 5% when stored at –20 °C for three months. Previously reported selenium dithiolates are unstable at neutral pH.²⁴ The characterization details described in the next sections correspond to solid **6** prepared under acidic conditions with excess selenite and with BDTH₂ added dropwise over several hours.

The as-isolated mixture of **6** and **9** has a melting point (mp) of 160–195 °C, which reduces to 150–155 °C after multiple washes with ethanol, acetonitrile, and ethyl acetate. Interestingly, the mp of the mixture is nearly identical to that of (tritylS)₂Se at 156–160 °C.²⁵ However, these values are lower than the mp of pure **9** at 180–183 °C.

The precipitated mixture of **6** and **9** decomposes to a red solid when heated, so **6** and **9** could not be isolated by distillation like other (RS)₂Se-containing mixtures (with R = 2-methyl-2-propanethiol, for example).¹⁸ Attempts to sublime **9** out of the mixture only resulted in decomposition to red Se(0). DMSO and pyridine are the only solvents capable of dissolving the product, which precludes separation of **6** and **9** by column chromatography.^{19,18,26}

The inductively coupled plasma optical emission spectroscopy (ICP-OES) analysis of the mixture indicates a 4:1 S/Se ratio as expected for a mixture of **6** and **9**. The differential scanning calorimetry (DSC) analysis had a small broad endothermic transition at 108.15 °C (H₂O) and a large endothermic transition at 150.15 °C corresponding to ΔH = 11.76 J/g at the mp of the mixture. Thermal gravimetric analysis (TGA) has a 2.3% weight loss at 136 °C and 80% weight loss at 550 °C. Thus, the compound decomposes

without elimination of ligand fragments at and well-above the melting temperature. Additionally, no loss of **9** is observed during heating.

The IR spectrum of the mixture of **6** and **9** has a few important differences from the IR spectrum of free **1**. The NH absorption that normally occurs around 3239 cm^{-1} is shifted to 3294 cm^{-1} and slightly broadened. The CS absorption at 699 cm^{-1} is reduced in intensity. Importantly, the SH absorption normally observed in free **1** is not present in the product. The SH peaks were also not observed in the IR spectra of BDT-Hg and BDT-Pb.⁷ The IR absorbances for the mixture of **6** and **9** are broadened but the same as the absorbances observed for pure **9**.

The ^1H NMR spectra of the solid mixture of **6** and **9** contains too many overlapping peaks, including overlap with the DMSO solvent peak, to make peak assignments. However, there are peaks in the aliphatic C–H region similar to free **1**. The major resonances in the ^{13}C NMR spectrum, 36.5 ppm (equivalent CH_2), 37.0 ppm (equivalent CH_2), 126.3 ppm, 128.4 ppm, 129.8 ppm, 134.5 ppm (aromatic), and 165.9 ppm (equivalent $\text{C}=\text{O}$) are consistent with the C_s symmetry of **6**. The ^{13}C NMR spectrum demonstrates that the carbons in the two cysteamine groups of **1** are equivalent, meaning that the compound is symmetric, probably with a C_2 rotational axis. This indicates that the product does not contain the asymmetric, oxygen-inserted compound BDT(S–Se–O–S) (**7**).

The ^{77}Se NMR spectrum of the product in DMSO- d_6 has a strong resonance at $\delta = 675$ ppm and a very weak resonance at $\delta = 774$ ppm. The ^{77}Se NMR spectra of the solids from all of the synthetic attempts consistently had only two resonances in the region of 600–800 ppm. The minor resonance at $\delta \approx 774$ ppm corresponds to elemental hexagonal selenium, which is found at $\delta = 794$ ppm in the solid-state ^{77}Se NMR spectrum.²⁷ The difference of 20 ppm is due to DMSO, which is known to coordinate Se(0). Additionally, the minor resonance did not begin to appear until about halfway through the NMR run, and when the sample was removed from the NMR probe, gray (hexagonal) selenium had precipitated.

The resonance at $\delta = 675$ ppm is consistent with values found in the literature for Se(II) with –S–Se–S– bonding (Table 1).^{28,29} For example, the ^{77}Se NMR of bis(cysteamine)-

Table 1. ^{77}Se NMR (ppm) of Compounds Related to **6** (25 °C)

compound	δ	solvent	reference
bis(cysteamine)selenide	653	D_2O	28
bis(L-cysteine)selenide	687	D_2O	28
bis(hydroethylthio)selenide	573	acetone- d_6	29
bis(<i>tert</i> -butylthio)selenide	687	CDCl_3	19

selenide has a resonance at 652.6 ppm.²⁸ This compound has the greatest similarity to BDT(S–Se–S) (**6**) since the SH groups in BDTH₂ originate from cysteamine. The ^{77}Se NMR data rules out the presence of tetravalent BDT–Se=O in the mixture since such compounds have ^{77}Se NMR resonances above 800 ppm.³⁰ For example, $(\text{CH}_3)_2\text{Se}=\text{O}$ has a chemical shift of 819 ppm.³⁰

2.2. BDTH₂ Combined with Selenate. No reaction occurs when BDTH₂ is combined with selenate. Almost all the initial weight of BDTH₂ was recovered by filtration as a white solid and was characterized as BDTH₂. To obviate the possibility

that **1** might have reduced selenate to selenite (albeit without precipitation), the Na_2SeO_4 was analyzed for selenite. Mercaptoethanol is used in the turbidimetric analysis of selenite based on reactions 1 and 4.²⁹ Cysteamine, which is also known to precipitate elemental selenium when combined with selenite at neutral and basic pH,²⁸ was used for the analysis. The filtrates from the combination of **1** and Na_2SeO_4 and a control sample, made with sodium selenate, were split into three aliquots: basic, acidic, and neutral. After addition of cysteamine there was no observation of elemental selenium precipitation or a red or gray colored suspension in any of the reaction filtrate aliquots or the control aliquots of sodium selenate. This qualitatively confirms that there is no reaction of **1** with selenate and that selenate is not reduced to selenite in the presence of thiols.

The absence of reactivity between selenate and **1** is in keeping with the hard–soft acid–base (HSAB) theory.^{31,32} The interaction of the soft thiol groups of **1** with the hard acid, selenate, are unfavorable. Selenite is a softer acid than selenate and will undergo a nucleophilic reaction with thiols. The Se(II) in **6** is even softer and so is readily reduced by thiols to Se(0). Additionally, selenate exists as the anion $[\text{HSeO}_4]^-$ at pH 0–2 and is dianionic $[\text{SeO}_4]^{2-}$ above pH 2.³³ The negative charge on selenate could prevent nucleophilic attack by the thiols in **1** through electrostatic repulsion. In contrast, selenite exists as neutral H_2SeO_3 from pH 0–2.5, which allows the dehydration reaction to take place.

2.3. Isolation of BDT(S–S) (9**) from the Precipitate Containing **6** and **9**.** The yellow mixture of **6** and **9** was decomposed to **9** and red Se(0) using aqueous sodium hydroxide. The Se(0) was made soluble by extraction with 1,3-diaminopropane followed by decantation from the insoluble material comprised of remaining Se(0), indicated by red coloration, and compound **9**. The small amount of the insoluble solid lost during each decanting step prevented an accurate quantification of **9** compared to the amount of beginning mixture. The Raman spectrum of **1** has a strong peak at 2563 cm^{-1} corresponding to the S–H bond. The Raman spectrum of the white decomposition product (**9**) does not have the S–H peak but a new strong peak at 511 cm^{-1} corresponding to the S–S group. The Raman spectrum of the **6** + **9** mixture was not possible to obtain because even the lowest laser power and short exposure times caused decomposition of **6** to red Se(0), which was observed in the microscope picture taken immediately after the analysis was attempted (Supporting Information, Figure S3).

2.4. Quantum Chemical Analysis of the Reaction of BDTH₂ (1**) with H_2SeO_3 .** Results of the quantum-chemical investigation are summarized in Tables 2 and 3, where Table 2 gives the energetics (both gas phase values and values for aqueous solution) for the reactions shown in Scheme 2 (for additional mechanistic details, see Scheme S1 of the Supporting Information). The table includes the energy difference at 0 K as well as enthalpy and Gibbs free energy differences at 298 K. Since some experiments were carried out in DMSO and water–alcohol solutions, energy differences were also calculated for these environments; however, the changes in the energy were relatively small. Therefore, the discussion will focus exclusively on the free energy differences $\Delta G(298)$ obtained in aqueous solutions.

Conformations and geometries for the molecules investigated are shown in Figures 3–7. Table 3 contains the calculated ^{77}Se NMR chemical shifts in the gas phase and

Table 2. Energetics of Reactions R1–R12

reaction ^b	gas phase ^a			water ^a		
	ΔE	$\Delta H(298)$	$\Delta G(298)$	ΔE	$\Delta H(298)$	$\Delta G(298)$
R1	-1.1	1.9	8.6	2.5	4.9	9.7
R2	-21.1	-20.8	-23.4	-20.5	-19.7	-21.4
R3	-21.1	-20.8	-22.1	-21.4	-20.8	-22.0
R4	-22.3	-18.8	-13.5	-18.9	-15.8	-12.3
R5	12.8	10.8	-0.7	9.1	7.5	-2.3
R6	-10.0	-9.4	-6.9	-7.6	-7.2	-6.0
R7	-0.8	-0.8	0.2	1.6	1.4	1.5
R8	-8.7	-9.3	-27.4	-12.1	-12.8	-31.2
R9	-20.7	-19.3	-26.9	-22.8	-21.7	-30.4
R10	8.6	8.5	7.5	8.3	8.2	7.4
R11	8.1	7.4	4.8	5.2	4.5	2.5
R12	4.0	4.3	3.6	4.7	4.8	4.7

^aAll values in kcal/mol. ^bSee Scheme 2 and text. Values obtained with ω B97X D/cc-pVTZ-PP calculations in the gas phase and in aqueous solution.

Table 3. Calculated ⁷⁷Se NMR Chemical Shifts

molecule	symmetry	δ ⁷⁷ Se (gas phase) ^a	δ ⁷⁷ Se (water) ^a
Me ₂ Se ^b	C _{2v}	0	0
H ₂ Se	C _{2v}	-223.2	-211.8
H ₂ SeO ₃	C ₁	1137.8	1167.3
2	C ₁	797.7	855.9
3	C ₁	1347.4	1320.6
4	C ₁	1023	1056.6
5	C _s	1048.9	1089.2
6	C _s	632.9	676.8
7	C ₁	1520.7	1619.8
8	C ₁	863.4	914.4

^aShifts are in ppm relative to the isotropic magnetic shielding value of Me₂Se and are calculated with the GIAO/B3LYP/cc-pVTZ method for both the gas phase and aqueous solution using geometries calculated for these environments. ^bMagnetic shielding values of 1894.8 (gas phase) and 1934.3 (water).

DMSO solution. Dipole moments and some important bond lengths are listed in Table S3 in the Supporting Information.

The computational structure of **1** (Figure 3) has S–C bond lengths of 1.822 Å, which compares well with the X-ray crystal structures of the two polymorphs of **1**. The C–S bond lengths in *syn*- and *anti*-BDTH₂ are 1.820 Å and 1.807 Å, respectively.³⁴ The quantum chemical calculations give $\Delta G(298) = 9.7$ kcal/mol for the formation of **2** (Figure 3 and Scheme 2, R1), but $\Delta G(298) = -12.3$ kcal/mol for the formation of **4** and -14.3 kcal/mol for the formation of **5** (reaction R4 or R4 + R5 in Scheme 2). The acyclic selenenic acid **3** is 21.4 kcal/mol more stable than diol **2**. Likewise, the hypothetical R₂Se(OH)₂ is unstable with respect to rearrangement to R₂SeO (ΔH values in kcal/mol for R = H (-2.8), Me (-3.4) and Ph (-11.1)).³⁵ This explains the absence of R₂Se(OH)₂ (with R = alkyl, aryl or thiol) compounds in the literature. The relatively long Se–O bonds in **2** and **3** result from the strong hydrogen-bonding interactions between the hydroxyl oxygen and protic hydrogens of the ligand.

The free energy of the hydrate **4** is 22.0 kcal/mol lower than that of diol **2**. However, homolytic cleavage of the Se–S bond in **2** (reaction A4 of Scheme S1 in the Supporting Information) has an energy close to 50 kcal/mol, whereas the heterolytic dissociation of this bond still requires somewhat more than 30 kcal/mol, thus making the overall reaction R2 leading to **3** energetically unfavorable. Selenenic acid compounds RSeOH

similar to **3** have been postulated as intermediates in the catalytic cycle of glutathione peroxidase.³⁶ However, they are unstable to condensation to seleninic acid, RSeO₂H, and RSe–SeR. The condensation was prevented in one example through the use of the sterically encumbered ligand *p*-*tert*-butylcalix[6]-arene. Crystallographic data for the selenenic acid group incorporated by bonding to a phenyl group in the macrocycle gives a Se–O bond length of 1.763 Å,³⁶ which is shorter than the calculated Se–O bond length of 1.826 Å in **3**. However, the selenium is bonded to carbon in the crystal structure rather than to sulfur as in **3**.

In the next step, either selenium oxide **4** (in hydrated form) or **5** is formed. In **5**, the Se=O group is directed toward the interior of the 14-membered ring where it can establish attractive H-interactions with one of the methylene H atoms (2.54 Å) and the benzene H atom (2.35 Å; Figure 4). Much stronger hydrogen-bonding interactions can be established in the monohydrate **4** with the water molecule connected by hydrogen bonds to the Se=O, one of the C=O groups, and a methylene H atom (Figure 4). Hence, energy and enthalpy are in favor of **4** by 12.8 and 10.8 kcal/mol, which is only slightly reduced in aqueous solution (9.1 and 7.5 kcal/mol, Table 1). Entropy leads to a change in the free energies in favor of **5** by 2.3 kcal/mol. It is noteworthy that hydrated **4** has the largest dipole moment, 9.62 D, in water (see Table S3 of the Supporting Information), compared to a value of 8.39 D for **5**. Thus, the solvation energy would be greater for **4** than it would be for **5**. Solvation however depends also on the dimensions of the cavity being formed for the solute, which is larger for **4** and accordingly reduces the solvation energy.

Selenoxide compounds similar to **4** and **5** (Figure 4), such as (RS)₂SeO and (RS)₂SeO⋯H₂O, are not known in the literature and are predicted to be unstable to isomerization (see Discussion below). This was observed experimentally with the attempted formation of (^tBuS)₂SeO by oxidation of (^tBuS)₂Se.¹⁹ This resulted in isomerization to ^tBuS–Se–O–S^tBu, which returns to (^tBuS)₂Se in the presence of two additional thiols. Five compounds of the general formula (ArCH₂S)₂Se=O were claimed,³⁷ but the limited characterization data could correspond to oxygen-inserted compounds, with a S–Se–O–S linkage. No Se=O bonding was identified. Selenoxides with Se–C rather than Se–S bonds are known, however. For example, (*p*-MeOC₆H₄)₂SeO and the hydrate (*p*-MeOC₆H₄)₂SeO⋯H₂O have been structurally characterized.³⁵ In these structures the Se–O bond lengths are the same, at

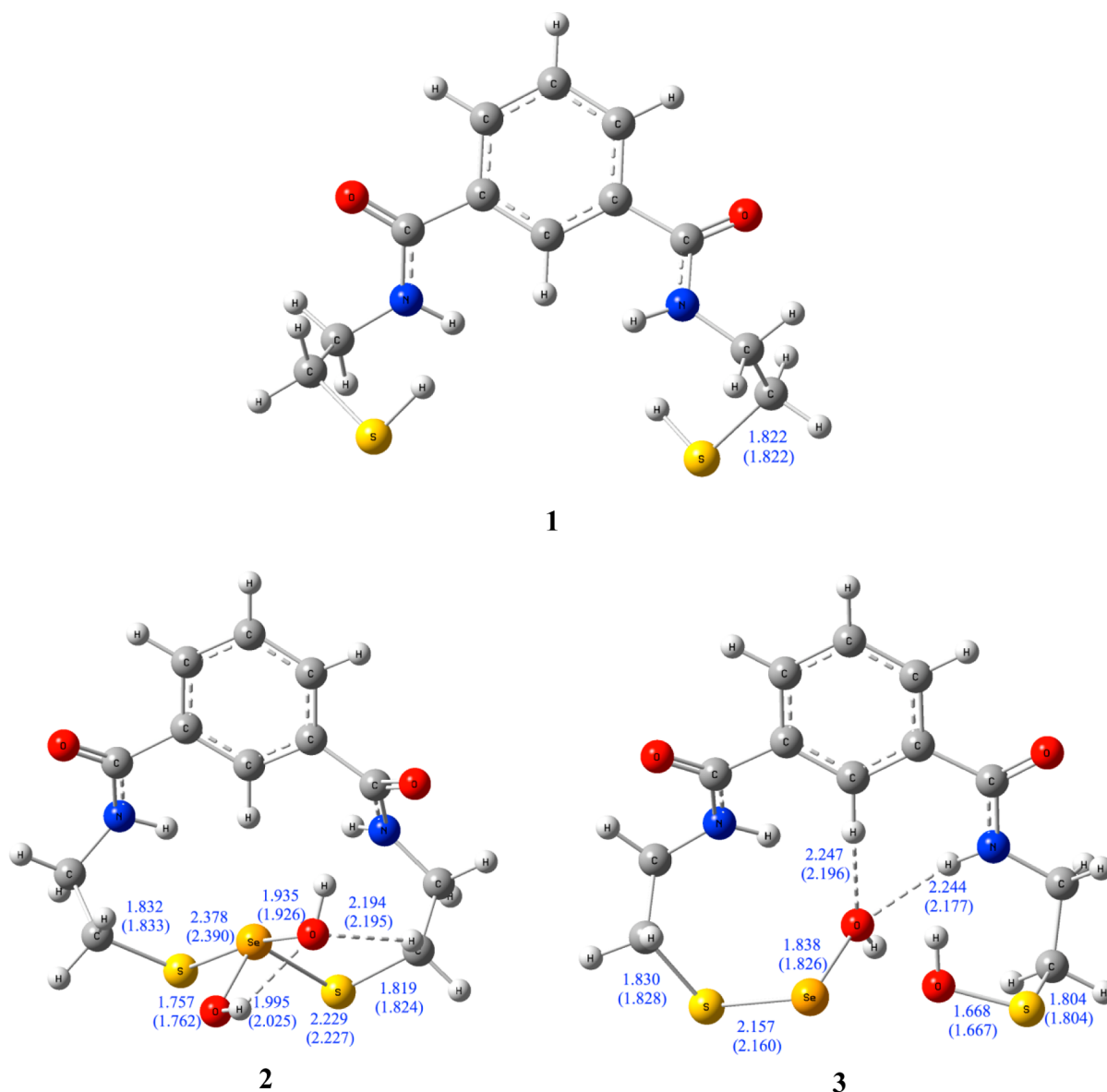


Figure 3. Calculated geometries (bond lengths in Å) and H-bond interactions of compounds 1, 2, and 3 according to ω B97X-D/cc-pVTZ-PP calculations (gas phase values; aqueous solution values in parentheses).

1.665 Å, indicating that no change occurs when this group forms a hydrogen bond to water. This distance is very similar to the Se–O distance in the calculated structure of 4 at 1.625 Å.

The intermediates 4 and 5 should be distinguishable by the ^{77}Se NMR chemical shifts at δ 1023 and 1049 ppm relative to dimethylselenide (Table 2). However, no experimental signal was observed in this range. Indeed, there are two other isomers of the selenium oxide 5, which can be generated by rearrangement at the selenium center. In aqueous solution selenosulfoxide 8 is the most stable of the three isomers. It can be formed by isomerization of 5 to 7 and a second isomerization of 7 to 8 leading to a $\Delta G(298)$ decrease of 6.0 kcal/mol.

Since the three isomers 5, 7, and 8 possess comparable free energies, large RIJCOSX-SCS-MP2/def2-TZVPP calculations were carried out, which suggest, somewhat surprisingly, that the 15-membered ring form with a polychalcogenide unit S–Se–O–S (7, Scheme 2 and Figure 5) is more stable by 1.5 (ΔE value) and 0.5 kcal/mol ($\Delta G(298)$ value). In the literature,

seleno-polysulfanes are known with two or more Se atoms; however, to the best of our knowledge, these do not include one or more oxygen atoms. The oxygen-inserted product ${}^t\text{BuSOSeS}{}^t\text{Bu}$ (reaction 3) has only been identified by ^1H NMR in an attempt to isolate $({}^t\text{BuS})_2\text{SeO}$ after oxidation with peracetic acid.¹⁹ No other characterization details have been published for an RSOSeSR compound.

The stability of 7 is a result of $\text{NH}\cdots\text{O}$ H-bonding and electrostatic attractions (Figure 5) as well as a strong anomeric delocalization of lone pair electrons in the S–Se–O–S chain of 7, which increases the bond strengths and enforces a helical arrangement with dihedral angles of 87, 142, 93, 79° for the C–S–Se–O–S–C–C chain starting with the dihedral angle C–S–Se–O. This effect is missing in 5. Also, considering that bonds involving oxygen are stronger than those involving S or Se, it is understandable that 7 is energetically somewhat more favorable than 5.

Molecules 4, 5, 7, and 8 represent equally likely intermediates in the reaction mixture because they possess

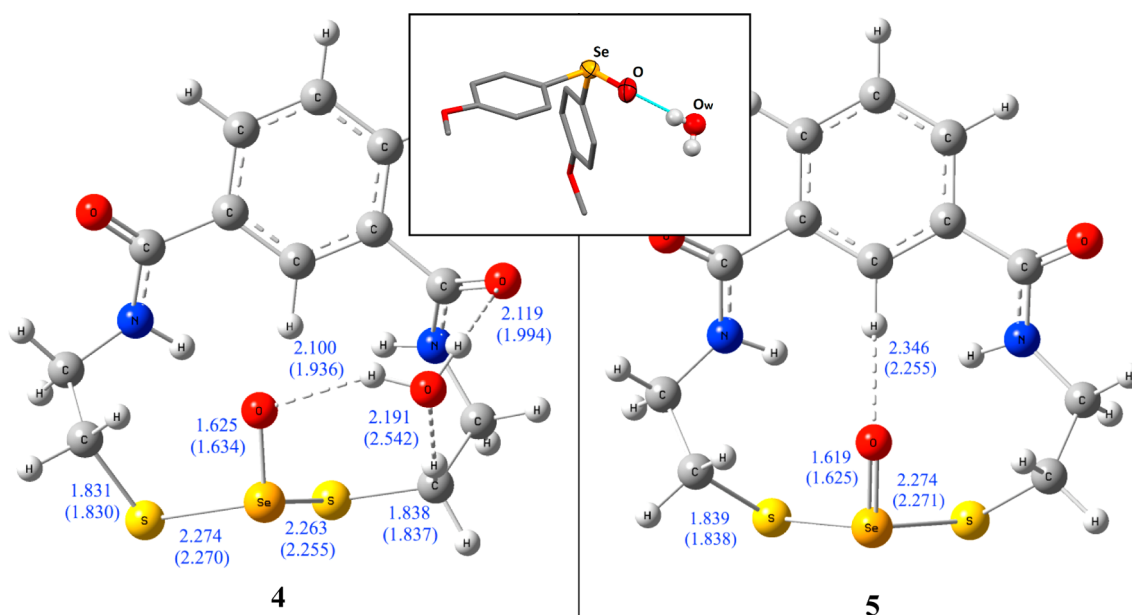


Figure 4. Calculated geometries (bond lengths in Å) and H-bond interactions of compounds (left) 4 and (right) 5 according to $\omega\text{B97X-D/cc-pVTZ-PP}$ calculations (gas phase values; aqueous solution values in parentheses). (inset) Crystal structure of $(p\text{-MeOC}_6\text{H}_4)_2\text{SeO}\cdots\text{H}_2\text{O}$ showing the hydrogen bonding similar to the hydrogen bonding calculated for 4. The inset structure was redrawn from reference 35 using the Mercury software program.

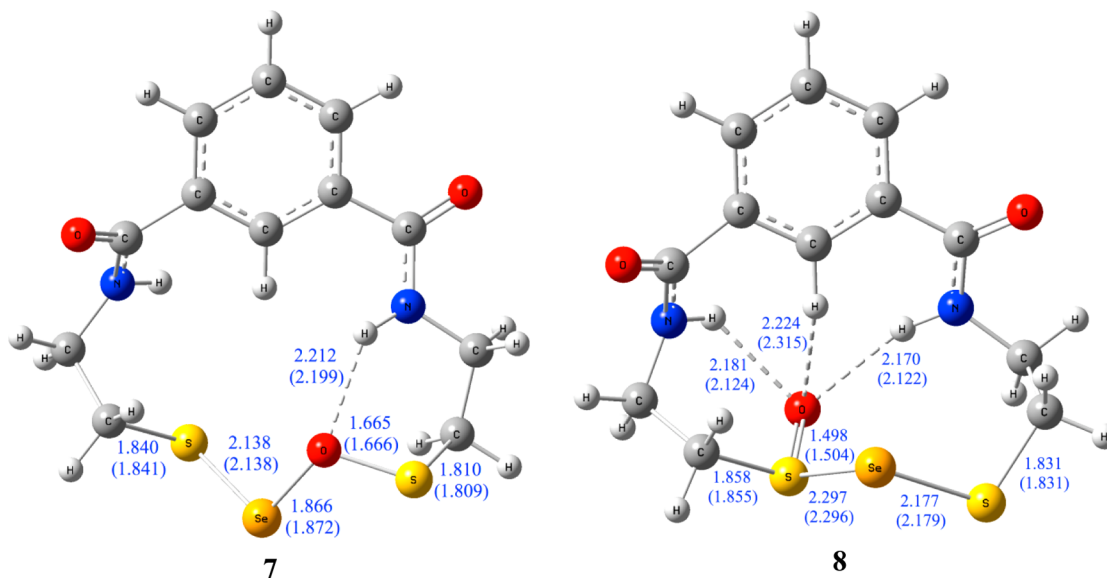


Figure 5. Calculated geometries (bond lengths in Å) and H-bond interactions of compounds (left) 7 and (right) 8 according to $\omega\text{B97X-D/cc-pVTZ-PP}$ calculations (gas phase values; aqueous solution values in parentheses).

comparable energies. The most likely reaction of selenium oxide 5 is with a second molecule of 1, which can lead to molecule 16 (most likely with H-bonding at $\text{Se}=\text{O}$), formation of RSeOH and a heterolytic cleavage of the $\text{S}-\text{Se}$ bond, hydride transfer to $\text{B}-\text{S}^+$, and formation of disulfane 9). Intramolecular condensation of 16 leads to selenide 6, producing a mixture of compounds in which the S/Se ratio is 4:1 (see reactions A6 and A7 of Scheme S1 in the Supporting Information).

Alternatively, in a five-membered transition state the acyclic molecule 17 could be formed, which could react with a third molecule of 1 in an intermolecular condensation reaction to yield molecule 18 (see Scheme S1, reactions A6 and A7, of the Supporting Information). Both 18 and 6 should have similar ^{77}Se NMR chemical shifts, but 18 would have a S/Se ratio of

6:1 (see Scheme S1 of the Supporting Information). Since the ICP-OES data gives a S/Se ratio of 4:1, this second path can be excluded. A similar reaction sequence can be expected for 7 (Scheme 2, R9). Hence, 5 or 7 (but less likely 8) reacts with another molecule of 1 to yield by reaction R8 or R9 (Scheme 2) in a clearly exothermic step ($\Delta G(298) = -31.2$ or -30.4 kcal/mol, Table 1) selenosulfane 6 and disulfane 9.

When comparing the calculated ^{77}Se NMR chemical shifts listed in Table 2, it becomes obvious that 6 is the only molecule that possesses a value of 633 ppm in the gas phase, which by deshielding effects in DMSO increases to 677 ppm, which is close to the measured value of 675 ppm. All other shift values are at least 180 ppm larger than the value for 6 (Table 2),

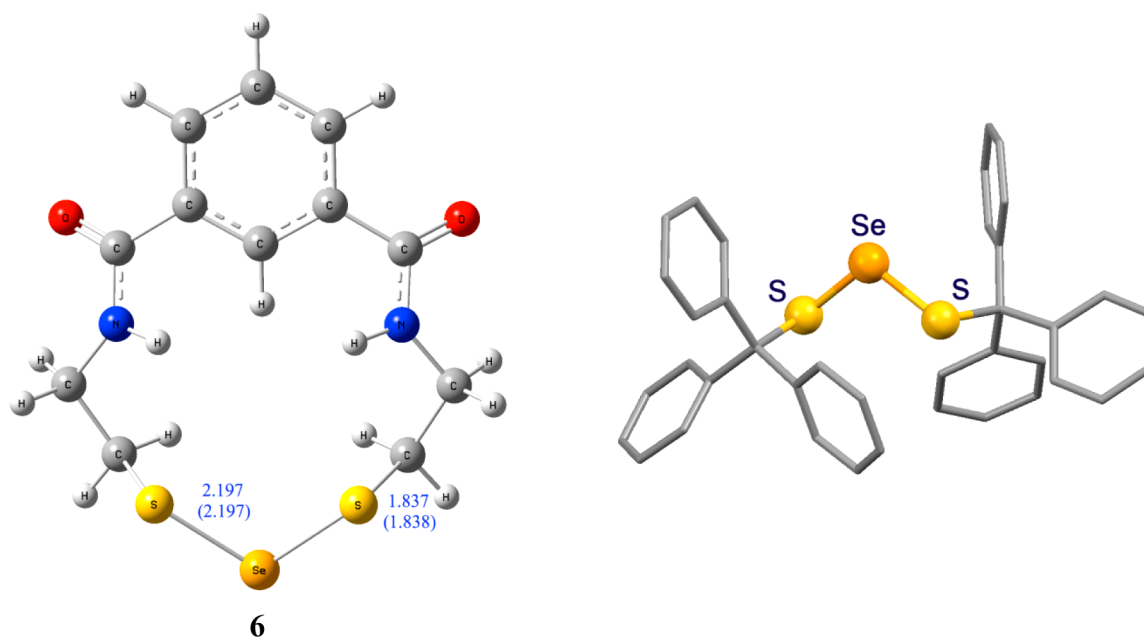


Figure 6. (left) Calculated geometry (bond lengths in Å) of compound **6** according to ω B97X-D/cc-pVTZ-PP calculations (gas phase values; aqueous solution values in parentheses). (right) The X-ray structure of (trityl) $_2$ Se from reference 25 redrawn with Mercury software using the single-crystal structural data.

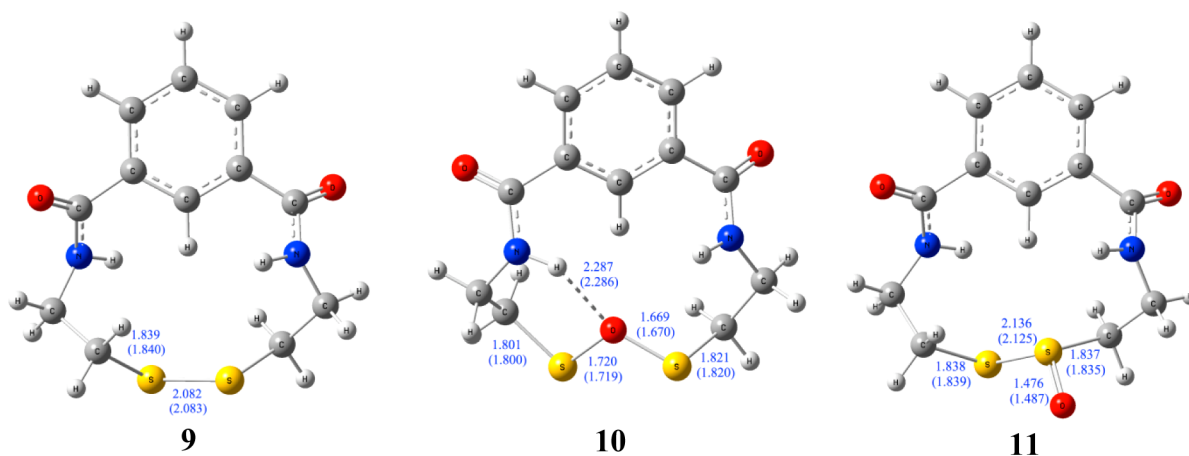


Figure 7. Calculated geometries (bond lengths in Å) and H-bond interactions of compounds **9**, **10**, and **11** according to ω B97X-D/cc-pVTZ-PP calculations (gas phase values; aqueous solution values in parentheses).

which verifies that **6** is the major product (beside elemental selenium) of the reaction.

The overall process, R4 + R8 in Scheme 2, is exothermic as reflected by $\Delta G(298) = -43.6$ kcal/mol. Molecule **6** possesses relatively short Se–S bonds of 2.197 Å, which do not change from the gas phase to DMSO or aqueous solution (see Table S3, Supporting Information), in line with the fact that its dipole moment is relatively small (2.73 D in the gas phase, 4.34 D in aqueous solution), indicating a somewhat smaller solvation energy. The Se–S bond lengths in **6** compare closely with those in (trityl) $_2$ Se, which are nonequivalent at 2.19 and 2.18 Å (Figure 6).²⁵ The S–Se–S bond angle in **6** (106.2°) is also similar to the angle in the X-ray structure (108.3°).

Previous investigations^{38,39} have indicated that elemental selenium implies the formation of transition states with tetra-coordinated Se (interaction of two molecules of **6**, two of **7**, or two of **8**), the elimination of Se $_2$ units and their polymerization leading to Se $_6$, Se $_7$, or (most likely) Se $_8$ (the red Se(0)

polymorph) as well as acyclic Se-polymers (the gray Se(0) polymorph). In this way the disulfane **9** or its oxidized analogues **10** and **11** are formed (Figure 7). In all cases, the Se $_8$ -producing reactions are endothermic overall ($\Delta G(298) =$ for R10, 7.4 kcal/mol; for R11, 2.5 kcal/mol; for R12 (**6** \rightarrow **9** + $1/8$ Se $_8$), 4.7 kcal/mol. It is possible however that the formation of red and gray selenium is autocatalytic in solution and requires much less energy.

3. EXPERIMENTAL SECTION

3.1. Reagents and Methods. BDTH $_2$ was prepared by condensation of isophthaloyl chloride (99% obtained from TCI America) with cysteamine hydrochloride (98% obtained from Acros Organics) following the literature method.⁴⁰ Sodium selenite (99%) was obtained from Sigma Aldrich, and sodium selenate (99.8%) was obtained from Alfa Aesar. All solvents used were obtained from AAPER. *d*⁶-DMSO (99.9% Cambridge Isotope Laboratories Inc.). Hydrochloric acid (reagent grade) and nitric acid (OmniTrace) were obtained from EMD. Sodium hydroxide (extra pure) was obtained

from Acros Organics. Instruments used to characterize BDT-Se included a melting-point apparatus (Melting-Temp, Laboratory Device), infrared spectrometer (Nicolet Avatar, Thermo Electron Corporation, KBr pellet), differential scanning calorimetry (TA Instruments DSC Q20), and thermal gravimetric analysis (TA Instruments TGA Q5000). Electron-impact (EI) ionization mass spectra were recorded at 70 eV on a ThermoFinnigan PolarisQ ion trap mass spectrometer. ^1H NMR (400.392 MHz), ^{13}C NMR (100.689 MHz), and ^{77}Se NMR (76.389 MHz) were obtained on a Varian INOVA instrument at 25 °C in DMSO- d_6 . ^1H NMR and ^{13}C NMR were referenced to solvent proton and carbon signal, respectively. ^{77}Se NMR spectra were referenced to an external standard of dimethyl selenide ($\delta = 0$ ppm). Varian Vista Pro CCD Simultaneous Inductively Coupled Plasma Optical Emission Spectrometer (ICP-OES) operating at 1.2 KW, with 10 s replicate read time, 15 L/min plasma flow, 1.5 L/min auxiliary flow, and 0.9 L/min nebulizer flow was used for ICP-OES data. Raman spectra were recorded on a Thermo Scientific DXR Raman Microscope with a 532 nm laser at 0.1 mW. ICP-OES was used to determine the sulfur/selenium ratio in BDT-Se. The compound (10 mg) was digested in triplicate. For the digestions, 5 mL of a 3:1 HCl/HNO₃ solution was added to the solid followed by heating for 2 h at 95 °C. A laboratory control sample (LCS) with a concentration of 20 ppm sulfur and 20 ppm selenium was digested in the same manner. After digestion one of the samples was spiked with 20 ppm sulfur and 20 ppm selenium. All samples, including a method blank and the LCS, were diluted to 50 mL with 1% HNO₃ after cooling to room temperature. Raw data and the calculation to obtain the S/Se ratio can be found in the Supporting Information.

3.2. Synthesis of BDT(S–Se–S) (6) under Acidic Conditions.

3.2.1. Excess Selenite. Sodium selenite, Na₂SeO₃ (2.70 g, 16 mmol), was dissolved in DI water (250 mL) and acidified to pH = 1 with HCl. A solution of BDTH₂ (2.28 g, 8 mmol) in EtOH (150 mL) was added to the selenite solution in 10 mL aliquots over 10 min. After the first aliquot of BDTH₂ was added a pale yellow precipitate formed, which began to agglomerate as additional aliquots were added. After stirring for 2 h the precipitate had agglomerated into a golf-ball sized mass. The reaction mixture was stirred for an additional 2 h, and the solid was isolated by filtration, washed with DI water (200 mL), acetone (100 mL), and allowed to dry in air. Yield = 2.7 g (92.5%). mp 160–195 °C (dec). IR (v, cm⁻¹): 3293 (–NH), 3067 (sp²-CH), 2926 (sp³-CH), 1638 (–C=O), 1535 (–NH), 699 (–CS). TGA (N₂, 10 °C/min ramp): onset 260 °C, 2.3% weight loss at 136 °C, 80% weight loss at 550 °C. DSC (15 °C/min ramp): a minor endothermic transition at 108.15 °C and a large endothermic transition at 150.15 °C corresponding to $\Delta H = 11.76$ J/g. ^{77}Se NMR (76 MHz, DMSO- d_6) δ (ppm): 675 (major) and 774 (minor). ^{13}C NMR (100 MHz, DMSO- d_6) δ (ppm): 36.5, 37.0, 126.3, 128.4, 129.8, 134.5, 165.9. ICP-OES gives a S/Se ratio of 4:1. ^1H NMR (400 MHz, DMSO- d_6) δ (ppm): 1.027, 2.950, 3.187, 3.625, 3.757, 3.875.

3.2.2. Excess BDTH₂. In an attempt to reduce the amount of disulfide byproduct, a shorter reaction was conducted without excess selenite. Sodium selenite, Na₂SeO₃ (0.153 g, 0.89 mmol), was dissolved in deoxygenated DI water (75 mL) and acidified to pH = 0.88 with HCl. A solution of BDTH₂ (0.50 g, 1.76 mmol) in absolute EtOH (40 mL) was added to the selenite solution, which immediately turned milky white. Upon addition there was a 7 °C increase in temperature, and the pH increased to 0.93. After stirring for 2 min the pH had increased to 1.14, and the solid began agglomerating as a pale yellow solid. The solution was stirred for an additional 8 min, and the solid was isolated by filtration, washed with DI water (50 mL), EtOH (50 mL), and allowed to dry under a stream of nitrogen. The final traces of solvent were removed under vacuum to obtain a pale white-yellow solid. Yield of 6 and 9 = 0.493 g. Mixture mp 150–195 °C (dec). With BDTH₂ (1) as limiting reagent (0.88 mmol) the reaction would theoretically yield 0.32 g of BDT(S–Se–S) (6) and 0.25 g of BDT(S–S) (9). Thus, the experimental yield, assuming a 1:1 mixture of 6 and 9, is 87%. Characterization data for the mixture of 6 and 9: IR (v, cm⁻¹): 3293 (–NH), 3063 (sp²-CH), 2918 (sp³-CH), 1634 (–C=O), 1527 (–NH), 687 (–CS); ^{77}Se NMR (76 MHz, DMSO-

d_6) δ (ppm): 677 (major) and 776 (minor). When the NMR tube was removed from the probe at the end of the run elemental selenium had precipitated as a gray solid.

A second reaction was conducted at a longer reaction time. Sodium selenite, Na₂SeO₃ (0.149 g, 0.86 mmol), was dissolved in 5% HCl (40 mL). BDTH₂ (0.53 g, 1.86 mmol) was added as a finely powdered solid. No yellow color was observed, and the solution was allowed to stir for 1 h before bringing the pH to 4 by the addition of NaOH. The solution was allowed to stir for 4 d open to air, and the solid was isolated by filtration, washed with DI water (50 mL), absolute EtOH (50 mL), and dried under a stream of nitrogen. The final traces of solvent were removed by vacuum to obtain a dark yellow solid. Mixture of 6 and 9: yield = 0.53 g (96% based on theoretical yields of 6 (0.31 g) and 9 (0.24 g). mp 115–125 °C (dec). IR (v, cm⁻¹): 3240 (–NH), 3056 (sp²-CH), 2926 (sp³-CH), 1636 (–C=O), 1533 (–NH), 697 (–CS). When dissolved in DMSO- d_6 elemental selenium precipitated as a gray solid within minutes.

3.3. Reactions that Produced Red Se(0).

3.3.1. Ambient pH. A solution of BDTH₂ (0.50 g, 1.76 mmol) in EtOH (25 mL) was added to a stirred solution of anhydrous sodium selenite (Na₂SeO₃, 0.32 g, 1.85 mmol) in DI water (25 mL). The reaction solution became maroon-colored after a few seconds, and a solid started precipitating. After stirring for 24 h the purple-colored solid was collected through filtration, washed with DI water (150 mL), EtOH (100 mL), and dried in air to yield 0.50 g of product as elemental selenium.

3.3.2. Ambient pH with BDTH₂ Added as a Solid. BDTH₂ (0.51 g, 1.79 mmol) was added to a stirred solution of anhydrous sodium selenite (Na₂SeO₃, 0.33 g, 1.90 mmol) in DI water (50 mL). The resulting compound turned light red after a few seconds. After stirring for 24 h the red solid was collected through filtration, washed with DI water (150 mL) and EtOH (100 mL), and dried under air, giving 0.53 g of product as elemental selenium.

3.3.3. Basic Conditions. Sodium selenite, Na₂SeO₃ (1.07 g, 6.19 mmol), was dissolved in DI water (130 mL) and basified to pH = 10 with NaOH. A solution of BDTH₂ (0.44 g, 1.55 mmol) in EtOH (100 mL) was added to the selenite solution in 10 mL aliquots over 10 min. After the first aliquot of BDTH₂ was added a pale yellow precipitate formed, and the suspension became rose-colored. As the suspension continued to stir, the solid became brick-red colored, indicating the presence of red Se(0).

3.4. Decomposition of BDT(S–Se–S) (6) under Basic Conditions.

3.4.1. Suspension in Water. Compound 6 (0.15 g, 0.4 mmol) was suspended in DI water (40 mL) and sonicated for 4 h to break the solid into a powder (some larger pieces remained in the powder). The pale yellow suspension was diluted to 760 mL with DI water and brought to pH = 13 with NaOH (4.0 g, 0.1 M) dissolved in DI water (200 mL) added in 50 mL aliquots over 20 min. No noticeable change occurred immediately after addition of NaOH, but after stirring for 2 h the suspension was pink colored. The suspension was stirred an additional 12 h and was then filtered to obtain a pale red solid containing some pieces of yellow 6.

3.4.2. Separation of BDT(S–S) (9) from BDT(S–Se–S) (6). A BDT(S–Se–S) and BDT(S–S) mixture (0.1183 g) was dissolved in DMSO (5 mL) to form a clear yellow solution. NaOH (5 mL of a 6 M solution) was added, and the solution formed two layers. The bottom colorless layer was removed, leaving a clear red solution. This was centrifuged at 8000 rpm for 5 min. The red supernatant was decanted, and the yellow/white precipitate was resuspended in DI water (5 mL). To this solution 1,3-diaminopropane (5 drops) and 6 M NaOH (1 drop) were added. This was centrifuged at 8000 rpm for 5 min. The supernatant was removed, and DI water (5 mL) was added to the precipitate along with 1,3-diaminopropane (5 drops) and 6 M NaOH (1 drop). This was centrifuged at 8000 rpm for 5 min and repeated several times until a white precipitate was obtained. The white precipitate was washed with DI water (5 mL), absolute EtOH (5 mL), ether (5 mL), and dried under a stream of nitrogen. mp 180–190 °C (dec); IR (v, cm⁻¹): 3238 (–NH), 3065 (sp²-CH), 2916 (sp³-CH), 1636 (–C=O), 1533 (–NH), 686 (–CS). Raman (v, cm⁻¹): 3304 (–NH), 3073 (sp²-CH), 2922 (sp³-CH), 1642 (–C=O), 1555 (–NH), 660 (–CS), 511 (S–S).

3.5. Combination of BDTH₂ with Na₂SeO₄ (Selenate).

3.5.1. Acidic Conditions. Sodium selenate, Na₂SeO₄ (0.335 g, 1.77 mmol), was dissolved in DI water (50 mL) and brought to pH = 1 with HCl. BDTH₂ (**1**) (0.255 g, 0.90 mmol) was added as a solid, and the solution was stirred for 24 h, resulting in a suspension having the color and consistency of unreacted **1**. The solid was isolated by filtration (0.217 g), washed, and characterized as unreacted **1**.

3.5.2. Ambient pH. Sodium selenate, Na₂SeO₄ (0.041 g, 0.21 mmol), was dissolved in DI water (25 mL). BDTH₂ (**1**) (0.251 g, 0.88 mmol) was added as a solid, and the solution of selenate with insoluble **1** was stirred for 24 h open to air. No reaction appeared to take place. A white solid was isolated by filtration (0.234 g) and characterized as BDTH₂. The filtrate was brought to 50 mL with DI water, and 10 mL aliquots were added to three separate test tubes. One of the aliquots was acidified with HCl, another aliquot was made basic with NaOH, and the third aliquot was not altered. A fourth aliquot, which was a control solution made by dissolving sodium selenate (0.040 g, 0.21 mmol) in DI water (50 mL), was treated in the same manner as the three reaction aliquots. Cysteamine was added to the three aliquots from the reaction filtrate and to the three aliquots from the control sample. There was no observation of elemental selenium precipitation in any of the aliquots.

3.6. Computational Methods. Different conformational forms of molecules **1**–**11** were investigated using density functional theory (DFT) with the long-range corrected hybrid exchange-correlation functional ω B97X-D that explicitly includes dispersion corrections.^{41,42} All DFT calculations were carried out with Dunning's correlation consistent, polarized valence triple- ζ basis set cc-pVTZ,^{43,44} which for Se was combined with an effective core potential for the innermost 10 electrons obtained by fully relativistic fitting, thus yielding a cc-pVTZ-PP (pseudopotential) basis set.⁴⁵ Sherill and co-workers⁴⁶ showed that ω B97X-D/cc-pVTZ calculations describe H-bonding energies and dispersion interaction such as π -stacking with an accuracy that comes close to that of the much more expensive CCSD(T) calculations.

Most molecules investigated contain a 14- or 15-membered ring that is relatively flexible and can adopt different conformational forms, which were systematically searched. In all cases, a complete optimization of the molecular geometry was carried out to obtain the most stable conformation. Then, the vibrational frequencies were calculated for each of the stationary points obtained so that the latter could be identified as minimum or first order saddle point. Vibrational, thermochemical, and entropy corrections were calculated to determine, besides energy differences ΔE at 0 K, enthalpy and free energy differences at 298 K, $\Delta H(298)$ and $\Delta G(298)$.

In the case of the isomers **5**, **7**, and **8**, calculations were repeated to verify results with the second-order Møller–Plesset (MP2) method utilizing (i) the resolution of the identity for the Coulomb part **J** and the chain of spheres approach for the exchange part **X**⁴⁷ and (ii) the spin-component scaled MP2⁴⁸ (abbreviated as RJCOSX-SCS-MP2) methodology, which is especially useful for large molecules. For the RJCOSX-SCS-MP2 calculations, all Hartree–Fock (HF) reference orbitals with an orbital energy larger than -4.0 hartree were correlated, and DFT geometries were used throughout. In the MP2 calculations, the default 2 (def2) valence triple- ζ with polarization functions (def2-TZVP) and the quadruple- ζ basis set with 2 sets of polarization functions (Def2-QZVPP)⁴⁹ were employed, where the latter led to more than 1600 basis functions.

Energy differences calculated for the gas phase can change when calculations are done in solutions. Therefore geometry optimizations for all conformational forms found for the gas phase were repeated in aqueous solution using a polarizable continuum,⁵⁰ the ω B97X-D functional, and the dielectric constant of water ($\epsilon = 79.8$ at 298 K).⁵¹ For the investigation of the NMR chemical shifts, the geometry optimization was repeated for DMSO ($\epsilon = 46.7$ at 298 K) and in some cases also for ethanol ($\epsilon = 24.55$ at 298 K) as a solvent.

The NMR shielding tensor of ⁷⁷Se was determined with the gauge-independent atomic orbital (GIAO) method using both the gas phase, DMSO, and aqueous solution geometries.⁵² As a suitable reference dimethylselenide, Me₂Se, was chosen to derive ⁷⁷Se NMR chemical shifts. For a small test set of selenium-containing molecules, for which

experimental ⁷⁷Se NMR chemical shifts have been reported, HF and B3LYP test calculations were carried out with several all-electron basis sets such as cc-pVnZ ($n = T, S$),⁵³ cc-pVnZ + 2 steepest primitive s -functions, uncontracted cc-pVTZ, and the universal gaussian basis set UGBS,⁵⁴ which is uncontracted in nature. Both HF and B3LYP revealed deficiencies in the prediction of ⁷⁷Se NMR chemical shifts. The best presentation was found by mixing up to 80% exact exchange into B3LYP in line with observations made for the calculation of magnetic shielding for second period nuclei.⁵⁵

For the purpose of getting a suitable reference value of the bond dissociation enthalpy at 298 K for the S–Se bond in HSeSH, G4 calculations were carried out.⁵⁶ For the quantum chemical calculations described in this work, the COLOGNE2012,⁵⁷ ORCA,⁵⁸ and Gaussian09 program packages⁵⁹ were used.

4. CONCLUSIONS

BDTH₂ (**1**) must be combined with excess selenite at pH ≈ 1 to avoid formation of red elemental selenium. Under these conditions, the reaction produces an immediate pale yellow precipitate that is a mixture of BDT(S–Se–S) (**6**) and BDT(S–S) (**9**) resulting from oxidation of **1**. The mixture is insoluble in water and all common organic solvents except DMSO and pyridine. The characterization data for **9**, isolated after sequential decomposition of **6** in the mixture of **6** and **9**, confirms the presence of a disulfide bond in **9**. Experimental and computational data also indicate that oxidation of **1** forms **9** rather than products having sulfoxide or sulfonate groups, which most likely would have been soluble in water. For example, the sulfonic acid derivative of cysteamine, H₂N-(CH₂)₂SO₃H, is very soluble in water.

The present work demonstrates that **1** reacts with selenite in essentially the same manner as free monodentate thiols; the thiols in **1** reduce Se(IV) to the Se(II)-containing product BDT(S–Se–S), which readily decomposes with heating or in moderately basic solution to **9** and red elemental selenium.

The quantum-chemical analysis of the mechanism of the reaction of selenite with **1** reveals that selenium oxide **4** (or **5**) is formed first, which then reacts with another equivalent of **1** to give **6** and **9**. The ⁷⁷Se NMR chemical shifts (measured or calculated) identify selenium dithiolate **6** as the major selenium-containing product. Compound **6** gains its stability from anomeric delocalization of electron lone pairs in the S–Se–S unit and hydrogen-bonding interactions involving the two amide groups. For the first time, a cyclic BDT compound containing the S–Se–S unit has been characterized.

BDTH₂ (**1**) can be used to precipitate selenite from acidic aqueous solutions either as BDT(S–Se–S) **9** or elemental solid selenium. Se(VI) must be reduced first to Se(IV) before adding **1** to the solution. Se(VI) is normally reduced by using concentrated HCl at elevated temperatures (80–100 °C),⁶⁰ which is a procedure that is difficult to carry out under wastewater purification conditions. The temperature and the concentration of HCl can be lowered when using suitable catalysts,^{60,61} but the conditions are such that the catalyst is difficult to recover. Reduction with thiourea is a milder technique, but the reaction takes up to 1 h to complete.⁶¹ These examples show that a reduction of Se(VI) to Se(IV) is in principle possible; however, it would have to be optimized for the specific purpose of reducing Se(VI) so that the Se(IV) could be removed after precipitation with **1**.

The interaction of selenite with thiols and dithiols is important in the mechanism of biological selenium toxicity. We demonstrate by ⁷⁷Se NMR and computational analysis that the dithiol BDTH₂ forms a two-coordinate compound (**6**) with

a S–Se–S linkage, but the compound is highly susceptible to decomposition through reduction of Se(II) to Se(0). In contrast, the lipoic acid (LA) derivatives, also containing a S–Se–S linkage, were reported to be “remarkably stable at neutral pH.”²⁴ While the two LA(S–Se–S) compounds were characterized by detection of ⁷⁵Se in the high-performance liquid chromatography, absorbance spectra, and mass spectroscopy, the handling did not decompose the products. Since the BDT and LA compounds will have similar anomeric stabilization and relatively little steric bulk, the difference in stability may be due to hydrogen-bonding in the LA compounds through the $-(\text{CH}_2)_4\text{COOH}$ and $-(\text{CH}_2)_4\text{COONH}_2$ substituents. Studies to address this possibility are in progress.

■ ASSOCIATED CONTENT

■ Supporting Information

This material is available free of charge via the Internet at <http://pubs.acs.org>.

■ AUTHOR INFORMATION

Corresponding Authors

*E-mail: dcremer@smu.edu. (D.C.)

*E-mail: datwood@uky.edu. (D.A.)

Notes

The authors declare no competing financial interest.

■ ACKNOWLEDGMENTS

The ICP-OES analyses were conducted in the University of Kentucky Environmental Research and Training Laboratory (ERTL; <http://ertl.uky.edu/>) with critical assistance provided by Tricia Coakley. Funding for this project was provided by the National Science Foundation Kentucky Experimental Program to Stimulate Competitive Research (NSF-KY-EPSCoR). Mass spectral data were obtained at the University of Kentucky Mass Spectrometry Facility. The computational investigation was financially supported by the National Science Foundation, Grant CHE 1152357. We thank SMU for providing computational resources.

■ REFERENCES

- (1) Reilly, C. *Selenium In Food And Health*; Blackie Academic and Professional: London, U.K., 1996.
- (2) Lemly, A. D. *Selenium Assessment and Aquatic Ecosystems: A Guide for Hazard Evaluation and Water Quality Criteria*; Springer-Verlag: Berlin, 2002.
- (3) Risher, J.; McDonald, A. R.; Citra, M. J.; Bosch, S.; Amata, R. J. *Toxicological Profile for Selenium*; Technical Report for the Agency for Toxic Substances and Disease Registry (ATSDR): Atlanta, GA, 2003.
- (4) Isakov, E. *Cutting Data for Turning of Steel*; Industrial Press, Incorporated: New York, 2009.
- (5) Gol'dshteyn, Y. E.; Mushtakova, T. L.; Komissarova, T. A. *Met. Sci. Heat Treat.* **1979**, *21*, 741.
- (6) Matlock, M. M.; Howerton, B. S.; Henke, K. R.; Atwood, D. A. *J. Hazard. Mater.* **2001**, *B82*, 55.
- (7) Matlock, M. M.; Howerton, B. S.; Atwood, D. A. *J. Hazard. Mater.* **2001**, *84*, 73.
- (8) Matlock, M. M.; Howerton, B. S.; Robertson, J. D.; Atwood, D. A. *Ind. Eng. Chem. Res.* **2002**, *41*, 5278.
- (9) Matlock, M. M.; Howerton, B. S.; Van Aelstyn, M.; Nordstrom, F. L.; Atwood, D. A. *Environ. Sci. Technol.* **2002**, *36*, 1636.
- (10) Matlock, M. M.; Howerton, B. S.; Atwood, D. A. *Water Res.* **2002**, *36*, 4757.
- (11) Matlock, M. M.; Howerton, B. S.; Atwood, D. A. *Adv. Environ. Res.* **2003**, *7*, 347.
- (12) Zaman, K. M.; Blue, L. Y.; Huggins, F. E.; Atwood, D. A. *Inorg. Chem.* **2007**, *46*, 1975.
- (13) Haley, B. E.; Gupta, N. N.; U.S. Patent 2013/0108605 A1, 2013.
- (14) Clarke, D.; Buchanan, R.; Gupta, N.; Haley, B. *Toxicol. Environ. Chem.* **2012**, *94*, 616.
- (15) Zou, W.; Filatov, M.; Atwood, D.; Cremer, D. *Inorg. Chem.* **2013**, *52*, 2497.
- (16) Painter, E. P. *Chem. Rev.* **1941**, *28*, 179.
- (17) Ganther, H. E. *Biochemistry* **1968**, *7*, 2898.
- (18) Kice, J. L.; Lee, T. W. S.; Pan, S.-T. *J. Am. Chem. Soc.* **1980**, *102*, 4448.
- (19) Kice, J. L.; Wilson, D. M.; Espinola, J. M. *J. Org. Chem.* **1991**, *56*, 3520.
- (20) Nogueira, C. W.; Zeni, G.; Rocha, J. B. *Chem. Rev.* **2004**, *104*, 6255.
- (21) Forastiere, D. O.; Borghi, E. B.; Morando, P. J. *Helv. Chim. Acta* **2007**, *90*, 1152.
- (22) Van Wart, H. E.; Scheraga, H. A. *J. Phys. Chem.* **1976**, *80*, 1812.
- (23) Barletta, R. E.; Gros, B. N.; Herring, M. P. *J. Raman Spectrosc.* **2009**, *40*, 972.
- (24) Self, W. T.; Tsai, L.; Stadtman, T. C. *Proc. Natl. Acad. Sci. U.S.A.* **2000**, *97*, 12481.
- (25) Ryan, M. D.; Abu-Yousef, I.; Rys, A.; Cheer, C.; Harpp, D. *Sulfur Lett.* **2003**, *26*, 29.
- (26) Kice, J. L.; Slebocka-Tilk, H. *J. Am. Chem. Soc.* **1982**, *104*, 7123.
- (27) Duddeck, H. *Prog. Nucl. Magn. Reson. Spectrosc.* **1995**, *27*, 1.
- (28) Rabenstein, D. L.; Tan, K.-S. *Magn. Reson. Chem.* **1988**, *26*, 1079.
- (29) Amaratunga, W.; Chaudry, O.; Milne, J. *Can. J. Chem.* **1994**, *72*, 1165.
- (30) Odom, J. D.; Dawson, W. H.; Ellis, P. D. *J. Am. Chem. Soc.* **1979**, *101*, 5815.
- (31) Pearson, R. G. *J. Am. Chem. Soc.* **1963**, *85*, 3533.
- (32) Pearson, R. G. *Chemical Hardness*; Wiley: Hoboken, NJ, 1997.
- (33) Takeno, N. *Atlas of E_r-pH Diagrams—Intercomparison of Thermodynamic Databases*; Technical Report for the National Institute of Advanced Industrial Science and Technology: Tokyo, May 2005.
- (34) Crystallographic data for the two polymorphs of **1** have been deposited with the Cambridge Crystallographic Data Center, Nos. 936262 (1-syn) and 936263 (1-anti). Electronic copies of this information may be obtained from the CCDC (E-mail: deposit@ccdc.cam.ac.uk or <http://www.ccdc.cam.ac.uk>).
- (35) Beckmann, J.; Duthie, A. Z. *Anorg. Allg. Chem.* **2005**, *631*, 1849.
- (36) Saiki, T.; Goto, K.; Okazaki, R. *Angew. Chem., Int. Ed.* **1997**, *36*, 2223.
- (37) Plano, D.; Baquedano, Y.; Ibanez, E.; Jimenez, I.; Palop, J. A.; Spallholz, J. E.; Sanmartin, C. *Molecules* **2010**, *15*, 7292.
- (38) Laitinen, R. S. *Acta Chem. Scand.* **1987**, *A41*, 361.
- (39) Zuckerman, J. J.; Hagen, A. P. *Inorganic Reactions and Methods, The Formation of Bonds to Group VIB (O, S, Se, Te, Po) Elements*; Wiley: Hoboken, NJ, 2009.
- (40) Atwood, D. A.; Matlock, M. M.; Howerton, B. S. U.S. Patent 6,586,600, 2003.
- (41) Chai, J. D.; Head-Gordon, M. *Phys. Chem. Chem. Phys.* **2008**, *10*, 6615.
- (42) Chai, J.-D.; Head-Gordon, M. *J. Chem. Phys.* **2008**, *128*, 084106.
- (43) Dunning, J. T. H. *J. Chem. Phys.* **1989**, *90*, 1007.
- (44) Woon, D. E.; Dunning, J. T. H. *J. Chem. Phys.* **1993**, *98*, 1358.
- (45) Peterson, K. A.; Figgen, D.; Goll, E.; Stoll, H.; Dolg, M. *J. Chem. Phys.* **2003**, *119*, 11113.
- (46) Thanthiriwatt, K. S.; Hohenstein, E. G.; Burns, L. A.; Sherrill, C. D. *J. Chem. Theory Comput.* **2010**, *7*, 88.
- (47) Kossmann, S.; Neese, F. *J. Chem. Theory Comput.* **2010**, *6*, 2325.
- (48) Grimme, S. *J. Chem. Phys.* **2003**, *118*, 9095.
- (49) Weigend, F.; Furche, F.; Ahlrichs, R. *J. Chem. Phys.* **2003**, *119*, 12753.

- (50) Tomasi, J.; Mennucci, B.; Cammi, R. *Chem. Rev.* **2005**, *105*, 2999.
- (51) Lide, D. R. *CRC Handbook of Chemistry and Physics: A Ready-Reference Book of Chemical and Physical Data*; CRC Press: Boca Raton, FL, 2000.
- (52) Cheeseman, J. R.; Trucks, G. W.; Keith, T. A.; Frisch, M. J. *J. Chem. Phys.* **1996**, *104*, 5497.
- (53) Wilson, A. K.; Woon, D. E.; Peterson, K. A.; Dunning, J. T. H. *J. Chem. Phys.* **1999**, *110*, 7667.
- (54) de Castro, E. V. R.; Jorge, F. E. *J. Chem. Phys.* **1998**, *108*, 5225.
- (55) Olsson, L.; Cremer, D. *J. Chem. Phys.* **1996**, *105*, 8995.
- (56) Curtiss, L. A.; Redfern, P. C.; Raghavachari, K. *J. Chem. Phys.* **2007**, *126*, 084108.
- (57) Kraka, E.; Filatov, M.; Zou, W.; Grafenstein, J.; Izotov, D.; Gauss, J.; He, Y.; Wu, A.; Polo, V.; Cremer, D. *COLOGNE2012*; Southern Methodist University: Dallas, TX, 2012.
- (58) Neese, F. *ORCA—an ab initio, Density Functional and Semiempirical program package, Version 2.9*; Max-Planck-Institut für Bioanorganische Chemie: Mülheim an der Ruhr, 2012.
- (59) Frisch, M. J. et al. *Gaussian 09*; Gaussian Inc.: Wallingford, CT, 2009.
- (60) Crompton, T. R. *Determination of Metals and Anions in Soils, Sediments, and Sludges*; Spon Press: Oxfordshire, U.K., 2001.
- (61) Chidambaram, S. *Recent Trends in Water Research: Hydrogeochemical and Hydrological Perspectives*; I. K. International Publishing House Pvt. Ltd., New Delhi, 2010.